fabricated by BESOI. These samples also showed that etch-stopping occurs and that the achieved film thickness agrees better with the expected thickness. However problems such as thickness uniformity and how can large areas be obtained, have to be investigated further before this technique can be applied. In this application the bond quality is important in terms of intrinsic voids and charges. Therefore, it is an advantage that the etch-stop layer is constructed after the fusion-bond step because of the benefit of having a free choice on which wafer the MIS oxide is going to be grown.

We have shown that an etch stop is achieved in an n-channel MIS fabricated on p-type silicon, biased so that an inversion and a depletion region are created. Therefore it is possible to fabricate an etch-stop layer without any external dopants and by that means achieve thin single-crystal silicon films, containing only the substrate dopant level. This etch-stop method can be used in the fabrication of BESOI islands. The results indicate that the area of these films can be large enough for VLSI electronics. Therefore, the applications for this etch-stop technique can span over a range from SOI fabrication to micromachined beams and membranes.

Acknowledgment

The authors specifically thank Professor B. Hök and Dr. H. Norde for helping us sort out the problems during this work, and ABB-Hafo for supplying us with silicon wafers and showing interest, to our reviewers who have put an impressive effort into reviewing this paper; and finally, the Swedish Board for Technical Development (NUTEK) for financial support.

Manuscript submitted Dec. 2, 1991; revised manuscript received Sept. 1, 1992.

The University of Uppsala assisted in meeting the publication costs of this article.

REFERENCES

1. W. P. Maszara, *This Journal*, **138,** 341 (1991).
2. N. F. Raley, Y. Sugiyama, and T. van Duzer, *ibid.*, **131,** 161 (1984).
3. H. G. Dura, J. Beltz, W. Mokwa, H. Vogt, and G. Zimmer, *Micromechanics,* Europe, Berlin (1990).
4. A. Söderbärg, *This Journal,* **139,** 561 (1992).
5. H. A. Wagganer, *Bell System Tech. J.,* **50,** 473 (1970).
6. E. D. Palik, V. M. Bermudez, and O. J. Glembocki, *This Journal,* **132,** 135 (1985).
7. E. D. Palik, *ibid.,* **132,** 871 (1985).
8. E. D. Palik, O. J. Glembocki, and I. Heard, *ibid.,* **134,** 404 (1987).
9. O. J. Glembocki, R. E. Stahlbush, and M. Tomkiewicz, *ibid.,* **132,** 145 (1985).
10. H. Seidel, L. Csepregi, A. Heuberger, and H. Baumgärtel, *ibid.,* **137,** 3612 (1990).
11. H. Seidel, L.Csepregi, A. Heuberger, and H. Baumgärtel, *ibid.,* **137,** 3626 (1990).
12. S. M. Sze, *Physics of Semiconductor Devices,* 2nd ed., p. 373, Wiley Interscience, New York (1981).

The Reaction Kinetics of Iron-Boron Pair Formation and Dissociation in P-Type Silicon

W. Wijaranakula*

Research and Development Department, SEH America, Incorporated, Vancouver, Washington 98682-6776

ABSTRACT

The reaction kinetics of iron-boron formation and dissociation in p-type silicon were investigated. The results indicate that the reaction kinetics depend strongly on the relative position of the ionization energy of interstitial iron and the Fermi level. At temperatures below a transition temperature where the ionization energy of interstitial iron is equal to the Fermi level, the iron-boron pairing reaction is dominated by the electrostatically enhanced recombination process between interstitial iron and substitutional boron. This pairing reaction is limited to the iron diffusion which may be described by the diffusion coefficient correlated by Weber.[8] At temperatures above the transition temperature, the concentrations of ionized and neutrally charged interstitial iron species are in equilibrium. The equilibrium reaction, which is facilitated by thermally excited electrons, gives rise to a deionization of the charged interstitial iron species and in turn causes the dissociation of the iron-boron pairs.

In integrated circuit (IC) device technology, transition metals, particularly iron (Fe), introduced during wafer processing and device fabrication cause either structural damage to the IC device or degrade its reliability during operation.[1] Characterization of electronic defects associated with interstitial iron (Fe_i), has been performed extensively during the past thirty years using techniques such as electron paramagnetic resonance (EPR)[2-4] and deep level transient spectroscopy (DLTS).[5-6] The EPR spectroscopy provides extensive information about the atomic and electronic configuration. Nevertheless, the shortcoming of this technique lies in the difficulty in determining the absolute concentration of the paramagnetic species.[7] The concentration of the neutral-charged interstitial iron (Fe_i^o) can be determined, for example, from the EPR intensity ratio between Fe_i^o and neutral-charged substitutional phosphorus (P_s^o) in n-type silicon of various doping levels.[8] In p-type silicon, however, the magnitude of the EPR intensity related to the positively charged species is proportional to the doping level of substitutional acceptors, when the concentration of the paramagnetic species is greater than the acceptor doping concentration.[8] In comparison to the EPR technique, the DLTS technique is a direct measurement of both the ionized Fe_i species and the electrically active defects associated with Fe complexes. Because the sensitivity of DLTS can be estimated from the concentration ratio between deep levels and shallow levels, on the order of 10^{-4}, a deep level concentration of 1×10^{11} cm^{-3} can be detected in p-type silicon typically used for fabricating the IC devices. Therefore, a combination of both techniques provides more complete information of both defect states and density.

From the EPR analysis, two charge states of interstitial Fe atoms, Fe_i^o and Fe_i^+, have been observed in p-type silicon contaminated with Fe after high-temperature quenching.[3] The presence of the Fe_i^+ species gives rise to an electrostatically enhanced interaction between Fe_i^+ and substitutional acceptors via an iron-acceptor pair formation. In silicon doped with boron, the defect ionization level associated with the $FeB^{o/+}$ species also may be characterized by the

* Electrochemical Society Active Member.

DLTS technique, and is identified to be at $E_v + 0.10$ eV; whereas that introduced by Fe_i^+ is at $E_v + 0.39$ eV, after correction with a measured temperature dependence of the capture cross section.[6] (The notation o/+ means that the defect is neutrally charged if the level is filled with an electron and positively charged if empty.) Thus, both Fe_i and FeB species exhibit hole traps in p-type silicon. An in-depth review of the electronic states and diffusion mechanism of Fe_i may be found elsewhere.[8]

In this paper the reaction kinetics of the FeB-pair formation and dissociation are discussed. Despite the simplifying assumptions, the results from the quantitative model of the FeB-pairing reaction provide some insight into the intricate coupling between the reaction kinetics of the FeB-pair formation and dissociation processes.

Theoretical

Theoretically, the reaction kinetics of the FeB-pair formation and dissociation in silicon doped with boron and containing Fe may be described by the expression

$$Fe_i^+ + B_s^- \underset{k_a}{\overset{k_d}{\rightleftarrows}} (FeB)^{o/+} \qquad [1]$$

where k_a and k_d are the constants for the association and dissociation reactions, respectively. A pairing reaction in Eq. 1 is diffusion-limited and can take place even at room temperature, due to the high diffusivity of the interstitial iron species. In general, the high diffusivity of transition metals is attributed to the difference in the elastic energies of the tetrahedral (T-site) and the hexagonal (H-site) sites.[9] Since an increase in the migration enthalpy (ΔH_m) of Fe_i has been observed in the absence of substitutional acceptors,[10] the diffusion of Fe_i^+ during the FeB-pairing reaction can be enhanced as a result of the coulombic force between ionized Fe_i and boron atoms. Because Eq. 1 cannot describe fully the reaction kinetics of FeB-pair formation and dissociation at high temperatures, where a significant amount of electrons are thermally excited, a deionization reaction of Fe_i^+ and a formation of $(FeB)^-$-pairs also need to be considered, such as presented by

$$Fe_i^+ + e \rightleftarrows Fe_i^o \qquad [2]$$

and

$$(Fe_iB_s)^o + e \rightleftarrows (FeB)^- \qquad [3]$$

In Eq. 3, the acceptor level of $(FeB)^-$-pairs is estimated to be on the order of $E_c - 0.55$ eV.[5] The electronically controlled reactions of interstitial iron in silicon has been examined previously by Kimerling and Benton.[11] The analysis has yielded an exponential relation between FeB-pair and Fe_i species in which most of the FeB-pairs are stable at temperatures up to 100°C; this is in contrast to other recent experimental observations using both DLTS[12] and EPR.[7]

From the EPR analysis,[7] all three iron species, including Fe_i^+, Fe_i^o, and FeB-pairs, are present in boron-doped silicon containing Fe, after high-temperature quenching. An isochronal annealing performed on as-quenched samples in the temperature range from room temperature up to 300°C results in a transformation from Fe_i^+ species to FeB-pairs. As observed from both EPR and DLTS measurements,[7,12] the transformation of the iron species exhibits three distinctive phases. In phase I, at temperatures below 100°C, the Fe_i concentration decreases with increasing isochronal annealing temperature, while the concentration of FeB-pairs increases. In phase II, at temperatures between 100 and 160°C, a recovery of the Fe_i species and a reduction in the FeB-pair concentration are observed as the isochronal annealing temperature increases. In phase III, at temperatures above 160°C, the concentrations of both Fe_i species and FeB-pairs decrease simultaneously as the isochronal annealing temperature increases. In addition to the above observation, during the phase I and II transformations, the sum of Fe_i and FeB-pair concentrations remains unchanged. The reaction kinetics associated with the phase I transformation have been interpreted as a result of the FeB-pair association reaction, while those with the phase II transformation are due to the dissociation reaction.[7,12] Thus far, this interpretation never has been verified theoretically.

Electrostatically enhanced pairing reactions.—Under the assumptions that all the interstitial iron atoms are ionized fully and the transformation of the Fe_i^+ species to FeB-pairs obeys first-order reaction kinetics, the rate of change in the Fe_i^+ concentration ΔC_{Fe}^+ as a result of the FeB-pair formation may be described by the differential equation

$$\frac{dC_{Fe}^+}{dt} = -\frac{1}{\tau_r}(C_{Fe}^+ - C_{Fe}^{+eq}) \qquad [4]$$

In Eq. 4, C_{Fe}^{+eq} is the concentration of the Fe_i^+ species which is in equilibrium with FeB-pairs and ionized boron atoms. t is the annealing time and τ_r is the rate constant of the pairing reaction. If it is assumed that ionized boron atoms are distributed homogeneously throughout the silicon matrix, the mean distance between ionized boron atoms is approximately equal to $C_B^{-1/3}$. Thus, for a diffusion-limited reaction, the rate constant $1/\tau_r$ may be written as

$$\frac{1}{\tau_r} = \frac{D_{Fe}}{L_{eff}^2} = D_{Fe}[C_B]^{2/3} \qquad [5]$$

In the above expression, L_{eff} is the effective diffusion length of the Fe_i^+ species, assumed to be approximately equal to the mean distance between boron atoms. D_{Fe} is the diffusivity of Fe_i^+ species,[8] which is given by

$$D_{Fe} = 1.3 \times 10^{-3} \exp\left(-\frac{0.68 \text{ eV}}{k_B T}\right) \qquad [6]$$

where k_B is the Boltzmann's constant and T is the absolute temperature.

The solution of Eq. 4 is governed by the initial condition, $C_{Fe}^+(t = 0) = C_{Fe}^{+I}$, where C_{Fe}^{+I} is the initial concentration of Fe_i^+ species prior to the isochronal annealing. After solving Eq. 4, the Fe_i^+ concentration then may be expressed as a function of annealing time as

$$C_{Fe}^+(t) = (C_{Fe}^{+I} - C_{Fe}^{+eq}) \exp\left(-\frac{t}{\tau_r}\right) + C_{Fe}^{+eq} \qquad [7]$$

Under the assumption that all the boron species are ionized fully, C_{Fe}^{+eq} may be expressed[11] by

$$C_{Fe}^{+eq} = \frac{C_{FeB}}{C_B 10^{-23} \exp\left(\frac{E_b}{k_B T}\right)} \qquad [8]$$

where C_{FeB} and C_B are the concentrations of FeB-pairs and ionized boron species, respectively. E_b is the binding energy of the FeB-pairs. The pair binding energy may be estimated using the expression

$$E_b = \frac{q^2}{\varepsilon r_1} \qquad [9]$$

where ε is the dielectric constant of silicon, q is the magnitude of electronic charge, and r_1 is the distance between the nearest T-site and the substitutional site, which is equal to 2.35 Å. Thus, in the case where an FeB-pair formation involves an interstitial iron atom, which is situated at the nearest T-site of the substitutional boron atom, the pair binding energy is estimated to be on the order of 0.52 eV.

According to the pairing reaction based upon the exponential decay Eq. 4, the concentrations of both ionized boron atoms and Fe_i^+ species decrease with increasing annealing time. Thus, the rate-change in the Fe_i^+ concentration, accounting for the reduction in both ionized boron atoms and Fe_i^+ species, must be described by a more intricate differential equation

$$\frac{dC_{Fe}^+}{dt} = D_{Fe}(C_{Fe}^+ - C_{Fe}^{+eq})(C_{Fe}^+ - C_B)^{2/3} \qquad [10]$$

For simplification, the solution of the first-order kinetics described by Eq. 7 may be considered; this simplification is justified by the results from Shepherd and Turner,[13] show-

ing that at least 80% for the FeB-pairing reaction follows a first-order law. As will be seen later, the FeB-pairing reaction also indeed obeys such first-order kinetics. The reaction kinetics of the FeB-pair formation can be evaluated based on the recombination rate and the pair binding energy. In Eq. 7 and 8, the recombination rate $1/\tau_r$ and E_b may be obtained from curve fitting to data from the EPR or DLTS measurements. If $1/\tau_r$ is known, D_{Fe} may be estimated from Eq. 5.

For comparison, the reaction kinetics of the FeB formation proposed by Nakashima *et al.*[14] are considered to be

$$C_{Fe}^{+}(t) = \frac{\alpha C_B}{\left[1 + \frac{\alpha C_B}{(C_{Fe}^{+i} - C_{Fe}^{+eq})}\right] \exp(\alpha k_a t) - 1} + C_{Fe}^{+eq} \quad [11]$$

where

$$\alpha = \frac{C_{Fe}^{+eq}}{C_B} + \frac{C_{Fe}^{t}(C_B - C_{Fe}^{t} + C_{Fe}^{+eq})}{C_B(C_{Fe}^{t} - C_{Fe}^{+eq})} \quad [12]$$

In this model, C_{Fe}^{t} is defined as the sum of Fe_i^+ and FeB-pair concentrations, assumed to be independent from the isochronal annealing period. The parameters, C_{Fe}^{+}, C_{Fe}^{+eq} and k_a may be obtained then from curve fitting of Eq. 11, provided the values of C_B and C_{Fe}^{t} are known. For steady-state conditions, the ratio between k_d and k_a is given by

$$\frac{k_d}{k_a} = \frac{C_{Fe}^{+eq}(C_B - C_{Fe}^{t} + C_{Fe}^{+eq})}{C_B(C_{Fe}^{t} - C_{Fe}^{+eq})} \quad [13]$$

In this model, the diffusion coefficient D_{Fe} is determined from the electrostatic interaction proposed by Kimerling *et al.*[15]

$$D_{Fe} = \frac{k_a k_B \varepsilon T}{q^2 C_B} \quad [14]$$

In Eq. 14, it is assumed that the charge on the Fe_i^+ species may be set at 1 q and the FeB-pairing reaction is diffusion-limited under consideration $k_a \propto D_{Fe}\, r_c$. In this expression, r_c is the capture radius for the Fe_i^+ species by ionized boron atoms.

Pairing reactions under local equilibrium conditions.— In addition to the reaction kinetics described in Eq. 1, the thermal ionization of the deep-level defects needs to be considered at high temperatures. According to Kittel,[16] the concentration of charged defects depends on the relative position of the defect ionization level. Since the Fe_i^o species are in local equilibrium with both isolated Fe_i^+ atoms and Fe_i^+ atoms which are associated in the FeB-pairs, the relationship between the concentrations of the Fe_i^+ and Fe_i^o species in p-type silicon may be written as

$$C_{Fe}^{o} = (C_{Fe}^{+} + C_{FeB}) \exp\left(\frac{E_F - E_{Fe}^{+}}{k_B T}\right) \quad [15]$$

where E_{Fe}^{+} is the defect ionization level, equal to 0.39 ± 0.02 eV,[6] and E_F is the Fermi level. In Eq. 15, all Fe_i^+ species are nearly ionized when $E_{Fe}^{+} - E_F > k_B T$. If $E_{Fe}^{+} - E_F < k_B T$, all defect sites have electrons trapped and become neutrally charged.[17] The temperature dependence of the Fermi level E_F is given by[18]

$$E_F(T) = E_i + k_B T \ln\left(\frac{p}{n_i}\right) \quad [16]$$

where E_i is the intrinsic Fermi level (approximately equal to $E_g/2$). Under the condition of space-charged neutrality, n_i and p are the intrinsic carrier concentration and the hole concentration in p-type silicon,[18] respectively, which are given by

$$n_i(T) = 2\left(\frac{2\pi k_B T}{h^2}\right)^{3/2} [m_e^* m_h^*]^{3/4} \exp\left(-\frac{E_g}{2k_B T}\right) \quad [17]$$

and

$$p = \frac{1}{2}[N_A - N_D + \sqrt{(N_A - N_D)^2 + 4n_i^2}] \quad [18]$$

In Eq. 17 and 18, m_e^* and m_h^* are the effective mass of electrons and holes, respectively; h is Planck's constant; and N_A and N_D are the total acceptor and donor concentrations, respectively. The bandgap energy E_g may be expressed as a function of absolute temperature as[19]

$$E_g(T) = 1.17 - \frac{4.73 \times 10^{-4} T^2}{T + 636} \quad [19]$$

In as-quenched p-type silicon contaminated with Fe, the Fe_i^o species are detected by the EPR technique.[7] Thus, the total concentration of iron C_{Fe}^{T}, which includes both electrically and nonelectrically active iron species, in as-quenched silicon is defined as

$$C_{Fe}^{T} = C_{Fe}^{+} + C_{Fe}^{o} + C_{FeB} \quad [20]$$

Substituting Eq. 15 into Eq. 20, the concentration of Fe_i^+ which is in equilibrium with the Fe_i^o species is then given by

$$C_{Fe}^{+} = \frac{C_{Fe}^{T}}{\exp\left(\frac{E_F - E_{Fe}^{+}}{k_B T}\right) + 1} - C_{FeB} \quad [21]$$

Figures 1a-c show the relative concentrations between Fe_i^+ and Fe_i^o as a function of the Fermi level at 50, 200, and 1000°C, respectively. For the Fermi level range below the ionization energy level of interstitial iron (E_v + 0.39 eV), the dominant iron species is Fe_i^+. In addition, the relative concentration between Fe_i^+ and Fe_i^o species decreases with in-

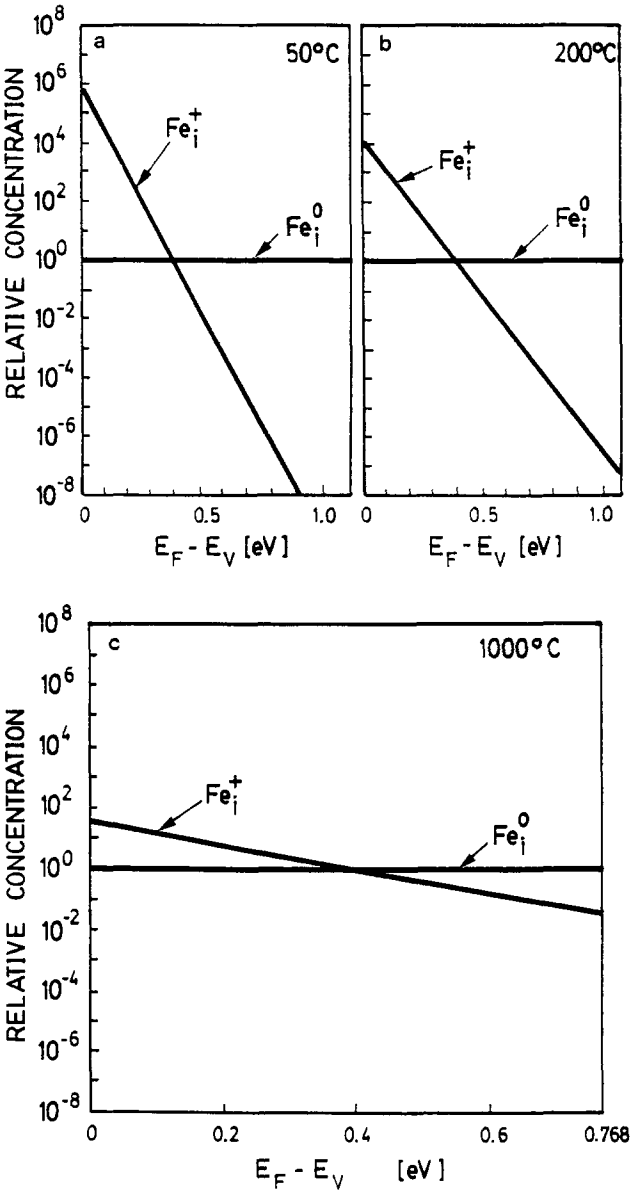

Fig. 1. Relative concentrations of Fe_i^+ and Fe_i^o as a function of the Fermi level; at (a) 50, (b) 200, and (c) 1000°C.

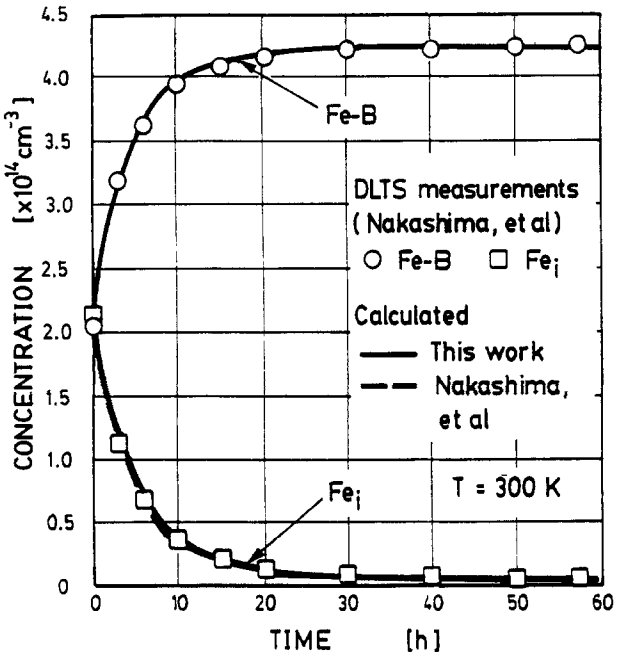

Fig. 2. Transformation from Fe_i^+ species to FeB-pairs at storage temperature T = 300 K.

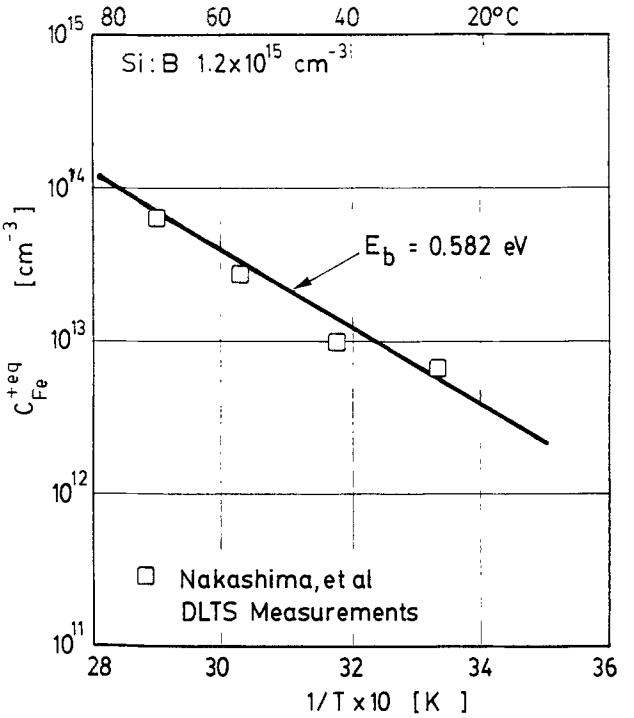

Fig. 3. The thermal equilibrium concentration of Fe_i^+ species in p-type silicon.

creasing annealing temperature. At high temperatures silicon becomes intrinsic and the position of the Fermi level approaches the midgap. Therefore, the concentrations of Fe_i^+ and Fe_i^0 species which are in equilibrium can be almost equal at high temperatures. Consequently, as-quenched samples contain both Fe_i^+ and Fe_i^0 species, thus in agreement with the EPR observation.

Evaluation of the Model

Time dependency of the electrostatically enhanced FeB-pairing reactions.—Figure 2 shows the transformation from Fe_i^+ species to FeB-pairs, as a function of storage time at 27°C.[14] The data were obtained from DLTS measurement performed on the aluminum-Schottky diodes. The samples were p-type, float-zone silicon having a <111> orientation and doped with boron to 1.2×10^{15} atom/cm^3. Fe was introduced into the samples by evaporating Fe onto the sample surfaces, followed by driven-in at temperatures between 950 and 1075°C in vacuum for times between 1.5 and 2.5 h. Subsequently, the samples were quenched to liquid nitrogen temperature. The calculated results, using this model Eq. 7 and the model proposed by Nakashima *et al.* are shown in Fig. 2. Equation 11 is in good agreement with the DLTS data. Fe_i concentration as determined by the DLTS consists of both Fe_i^0 and Fe_i^+ species. At 27°C, according to Eq. 15, the concentration of Fe_i^0 species, relative to the Fe_i^+ concentration, however, is negligible. Therefore, the Fe_i concentration in as-quenched samples as determined by the DLTS may be assumed to be attributed primarily to the Fe_i^+ species. The parameters used for the curve fitting are summarized in Table I. Interestingly, however, the recombination rate $1/\tau_r$ obtained from this model corresponds well with the association rate k_a. In Table I the diffusivity of Fe_i^+, calculated using the electrostatic interaction model

Table I. Summary of the results from the curve fitting.

References	C_{Fe}^{+eq} ($\times 10^{12}$ cm^{-3})	E_b (eV)	k_a ($\times 10^{-5}$ s^{-1})	τ_r	D_{Fe} Eq. 6 ($\times 10^{-15}$ cm^2/s)	D_{Fe} Eq. 14 ($\times 10^{-15}$ cm^2/s)
Nakashima *et al.*[14]	5.94	0.582	6.70	4.87	4.31	9.30
Ryoo and Socha[20]	0.09	0.581	2.18	2.14	2.14	3.57
Gao[22]	0.04	0.604	1.07	1.12	2.50	5.84

Eq. 14, is almost twice as high as that calculated using the simple diffusion model Eq. 5.

In Fig. 3, the equilibrium concentrations C_{Fe}^{+eq} derived from DLTS measurements[13] are plotted as a function of inverse temperature. The data were fitted to the Arrhenius equation obtained by substituting C_{FeB} in Eq. 8 with Eq. 21

$$C_{Fe}^{+eq} = \frac{C_{Fe}^{T}}{\left[1 + C_B 10^{-23} \exp\left(\frac{E_b}{k_B T}\right)\right]\left[1 + \exp\left(\frac{E_F - 0.39\ \text{eV}}{k_B T}\right)\right]} \quad [22]$$

In Eq. 22, C_{Fe}^{T} in as-quenched samples is given as 4.3×10^{14} cm^{-3}.[14] From the curve fitting, E_b is equal to 0.582 eV, in correspondence with the model of two electrostatically bound point defects.[11]

Figure 4 shows two sets of the DLTS data obtained from p-type CZ silicon with varying Fe surface contamination. Silicon samples used by Ryoo and Socha[20] were doped with boron to 3×10^{14} atom/cm^3. The Fe surface contamination was driven-in by a 15 min anneal at 1100°C, which was followed by a water quench. Subsequently, as-quenched samples were stored at room temperature (approximately 295 K) for one month to allow a complete transformation from Fe_i^+ species to FeB-pairs. The DLTS measurements were performed on titanium Schottky diodes. Prior to the initial DLTS measurement, samples were heated at 200°C for 2 min to dissociate the FeB-pairs into the Fe_i^+ species. Following such a dissociation anneal, the samples were quenched rapidly to room temperature to prevent the reverse reaction.[21]

Silicon samples used by Gao[22] were doped with boron to 1×10^{15} atoms/cm^3. The samples were first oxidized in dry oxygen ambient at 1000°C for 200 min and then air-cooled to room temperature. The DLTS measurements were performed on aluminum Schottky diodes after a 3-min anneal at 210°C. After the dissociation anneal, the samples were quenched in water. The parameters used for the curve fitting for both sets of the DLTS data are summarized in Table I. To fit the DLTS data in Fig. 4 using the model proposed by Nakashima *et al.*, an assumption had to be made that the total concentration of electrically active iron species C_{Fe}^{t} consists of 95% Fe_i^+ and 5% FeB-pairs after quenching. In general, the fitting parameters in Table I obtained from both models are in good agreement with each

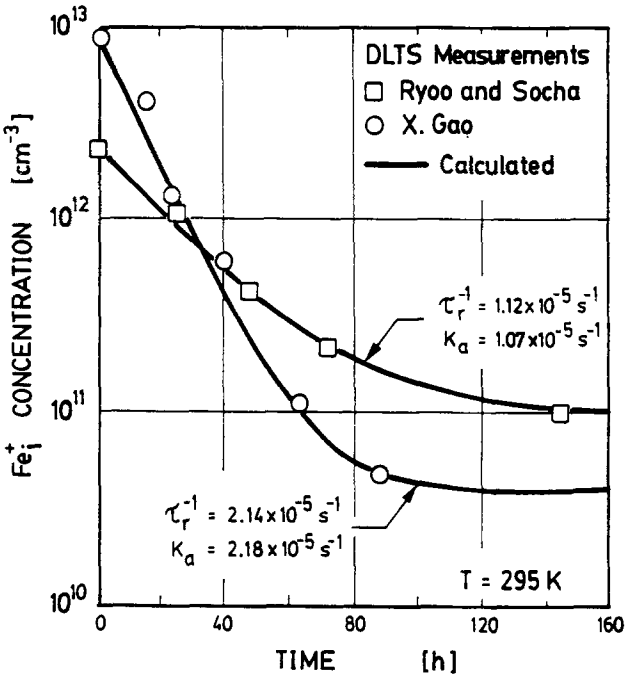

Fig. 4. Transformations from Fe_i^+ species to FeB-pairs at T = 295 K.

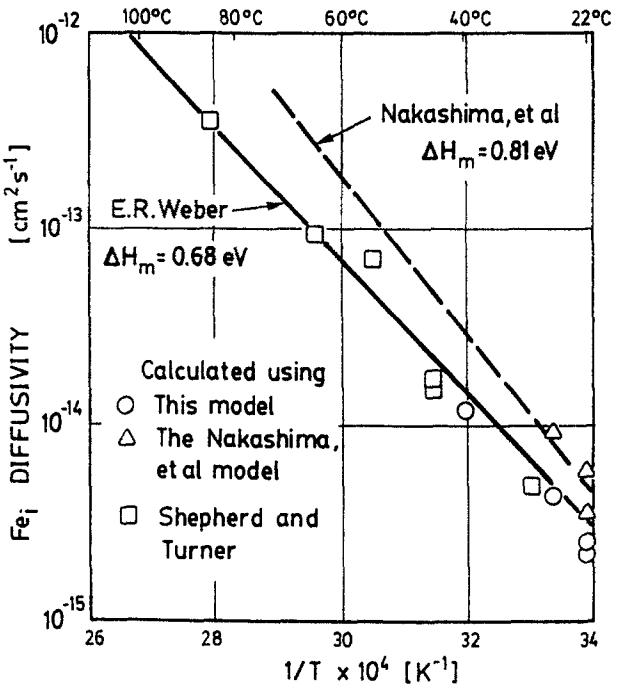

Fig. 6. The diffusivity of interstitial iron as a function of inverse temperature.

other. Similar to the previous observation, the recombination rate $1/\tau_r$ determined from the first-order decay equation is in good agreement with the association rate, k_a, derived from the rate reactions, Eq. 11.

Figure 5 shows the EPR data related to the Fe_i^+ species obtained from Fz, p-type silicon samples isochronally annealed at 40°C for times up to 200 min.[7] The boron doping concentration was given as 2.9 × 10^{15} atom/cm^3. Iron was introduced into the samples by placing the samples, along with a piece of high-purity Fe wire, into a sealed and evacuated quartz capsule. The capsule was then heated at 1300°C for 1 h and then quenched in ice water. As-quenched samples were stored in liquid nitrogen until the

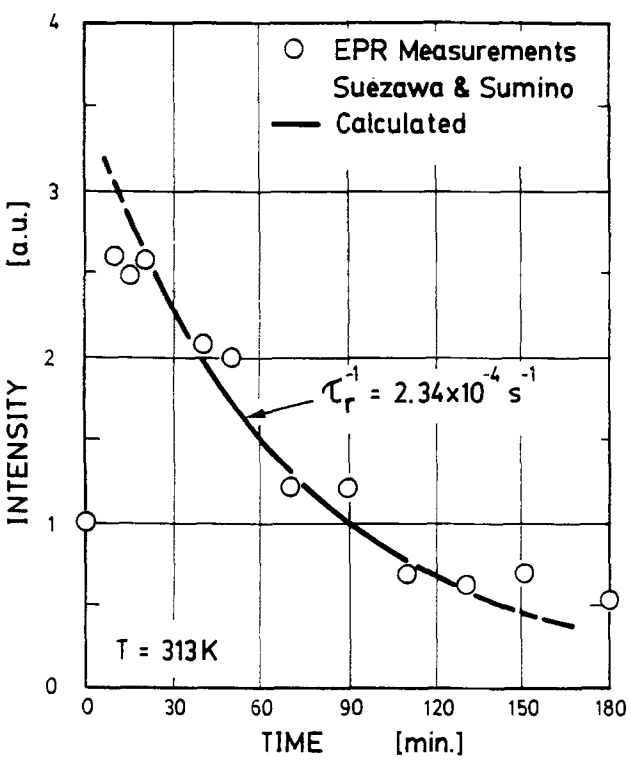

Fig. 5. EPR intensity related to Fe_i^+ species as a function of time T = 313 K.

EPR measurement was carried out. Because the determination of the absolute concentration value of the Fe_i^+ species was not performed, the EPR intensity related to the Fe_i^+ species was normalized to the intensity from an as-quenched sample. In contrast to the DLTS results shown in Fig. 2 and 4, the EPR intensity rises rapidly during the initial stage of the annealing process. This phenomenon was interpreted to be due to the thermal ionization of Fe_i^0 species in response to an increase in the concentration of the thermally excited electrons.[7] From the curve fitting, $1/\tau_r = 2.34 \times 10^{-4}$ s^{-1}. The normalized EPR intensities related to Fe_i^+ species in the as-quenched sample and the pair binding energy are 3.5 and 0.586 eV, respectively. The EPR data shown in Fig. 5 cannot be fitted to Eq. 11 because the absolute concentration of Fe_i^+ species is unknown. Nevertheless, good agreement may be obtained when the recombination rate $1/\tau_r$ is compared to k_a (as determined by the DLTS measurement on a Fe-doped p-type silicon sample annealed at 42°C),[14] equal to 3.0 × 10^{-4} s^{-1}. From the curve fitting, the diffusivity of the Fe_i^+ species at 40°C is 1.17 × 10^{-14} cm^2/s, in agreement with the iron diffusivity correlated by Weber,[8] equal to 1.47 × 10^{-14} cm^2/s.

In Fig. 6, the calculated diffusivities of the Fe_i^+ species using this model and the model proposed by Nakashima *et al.* are plotted as a function of inverse temperature. Along with the data, the Fe_i^+ diffusivities derived from the resistivity measurements by Shepherd and Turner[13] also are plotted. In Fig. 6, the solid line represents the iron diffusivity as correlated by Weber[8] while the broken line is the diffusivity given by Nakashima *et al.*[14] The migration enthalpy reported by Nakashima *et al.* is 0.81 eV, and thus is higher than that in Eq. 6, giving 0.68 eV. The deviation in the migration enthalpies and hence the diffusion coefficient may be due to the equations used for calculating the diffusivity. In Fig. 6, the diffusivities derived from this model correspond with the iron diffusivity correlated by Weber.[8] Thus, the Fe_i^+ diffusivity Eq. 6 is used in the next calculation. Substituting Eq. 5 into Eq. 7, the Fe_i^+ concentration in Eq. 7 may be expressed as a function of absolute temperature, time, and boron concentration as

$$C_{Fe}^{+}(t) = (C_{Fe}^{+I} - C_{Fe}^{+eq}) \exp\left[-1.3 \times 10^{-3}\, t [C_B]^{2/3} \exp\left(-\frac{0.68\ \text{eV}}{k_B T}\right)\right] + C_{Fe}^{+eq} \quad [23]$$

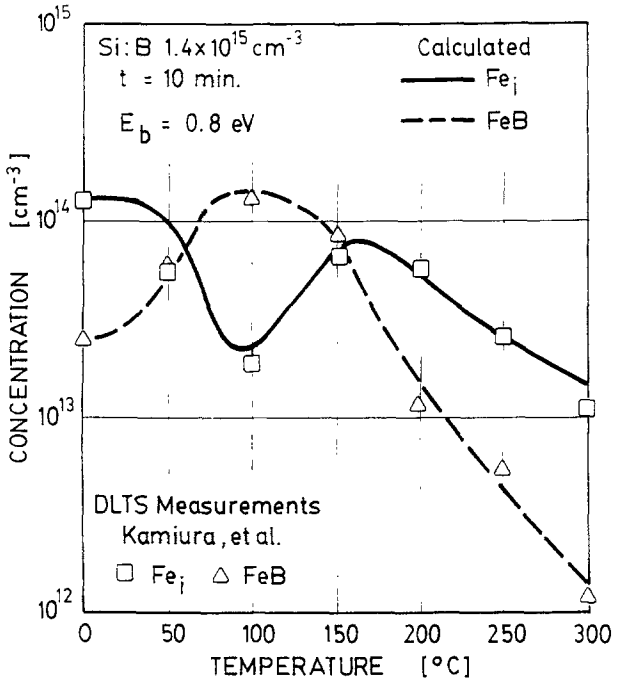

Fig. 7. Isochronal transformation from Fe_i^+ species to FeB-pairs after 10 min annealing.

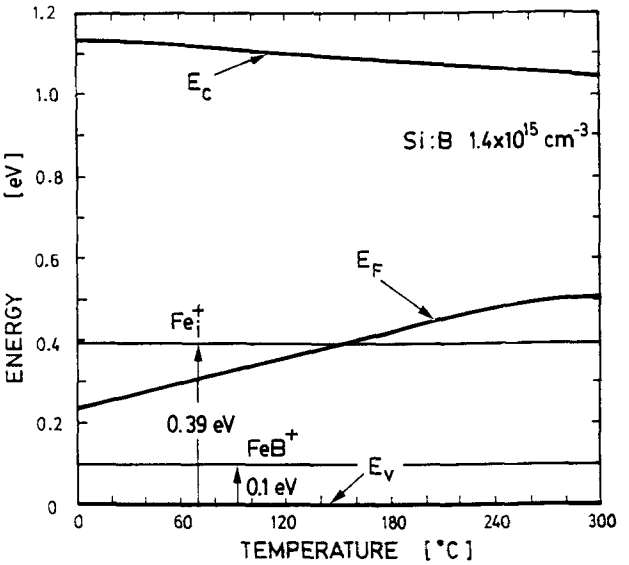

Fig. 8. The position of the Fermi level as a function of temperature for silicon doped with boron to 1.4×10^{15} cm^{-3}.

In Eq. 23, the first term approaches zero with increasing temperature and at temperatures $T < (E_F - E_{Fe}^+)/k_B$, $C_{Fe}^+(t) = C_{Fe}^{+eq}$. From the above expression, the concentration of FeB-pairs formed during the annealing period t may be calculated using the relationship

$$C_{FeB}(t) = C_{Fe}^I - C_{Fe}^+(t) \quad [24]$$

Thus, the total concentration of FeB-pairs in the sample after annealing may be written as

$$C_{FeB}^T = C_{FeB}^I + C_{FeB}(t) \quad [25]$$

where C_{FeB}^I is the initial concentration of FeB-pairs in as-quenched samples. The above expression implies that the FeB-pair dissociation occurs when $C_{FeB}(t) < 0$.

Temperature dependency of the FeB-pairing reactions.— In Fig. 7, the concentrations of Fe_i^+ species and FeB-pairs, as determined by the DLTS measurements, are plotted as a function of temperature.[11] The data were obtained from (111) CZ silicon doped with boron to 1.4×10^{15} atom/cm^3. Fe was introduced into the samples by evaporating Fe on the sample surfaces. Subsequently, the samples were annealed at 1000°C in argon for 1 h and then quenched in water. The DLTS measurements then were performed on titanium Schottky diodes, after the samples received a 10 min isochronal anneal in the temperature range between 50 and 300°C. From the DLTS measurements, C_{Fe} (Fe_i^+ and Fe_i^o) and C_{FeB}^I in as-quenched samples are 1.3×10^{14} and 2.35×10^{13} cm^{-3}, respectively. Thus, C_{Fe}^T is equal to 1.54×10^{14} cm^{-3}.

Prior to the curve fitting, the transformation temperature where the Fermi level is equal to the ionization energy of Fe_i^+ species is determined. In Fig. 8, the relative position of the Fermi level to the ionization energies of Fe_i^+ species and FeB-pairs (based on the given boron doping concentration of 1.4×10^{15} cm^{-3}) is calculated and plotted as a function of temperature. From Eq. 15, at temperatures below 120°C where $E_{Fe}^+ - E_F > kT$, nearly all Fe_i^+ species are ionized. At temperatures above 191°C, where $E_F - E_{Fe}^+ > kT$, all Fe_i^+ species which are not in thermal equilibrium with Fe_i^o have electrons trapped and become neutral. The transition temperature at which $E_{Fe}^+ = E_F$ is 153°C. The DLTS data in Fig. 7 are fitted to the expressions; C_{Fe} (DLTS) = $C_{Fe}^+ + C_{Fe}^o$ and C_{FeB} (DLTS) = C_{FeB}^T. At temperatures below 153°C, where the pairing reaction is dominated by the electrostatically enhanced recombination process, C_{Fe}^+ and C_{Fe}^o may be calculated from Eq. 23 and 15, respectively, while C_{FeB}^T may be determined from Eq. 25. At temperatures above 153°C, the equilibrium between Fe_i^+ and Fe_i^o species prevails. Thus, C_{Fe}^+ may be determined from Eq. 22.

The DLTS results in Fig. 7 represent only an average concentration of the defects in the depletion layer, approximately 3 μm for the reverse bias and pulse voltage of 5 V.[11] In the case where a large concentration gradient is present in the depletion layer, *e.g.*, out-diffusion profile, the defect concentration as determined by the DLTS may represent the integrated defect concentration within the depletion layer. Thus, for a fast-diffusing species such as iron, the effect of the Fe_i out-diffusion on the concentration gradient of the defect species at the surface region needs to be considered, particularly during an annealing in the temperature range above 100°C.[23] The Fe_i concentration as a function of depth may be calculated using the error function equation

$$C_{Fe}(x) = C_{Fe}(0) + [C_{Fe}(\infty) - C_{Fe}(0)] \operatorname{erf}\left(\frac{x}{2\sqrt{D_{Fe}t}}\right) \quad [26]$$

where $C_{Fe}(0)$ is the surface concentration, assumed to be equal to the thermal equilibrium concentration of iron.[8] $C_{Fe}(\infty)$ is the bulk iron concentration. From the curve fitting, E_b is 0.8 eV. In the curve fitting, it is assumed that the Fe_i concentration calculated at x = 1.5 μm or one-half the depletion layer width represents the integrated Fe_i concentration in the depletion layer during the reverse bias and pulse voltage of 5 V. The results from the calculation with E_b = 0.8 eV at temperatures above 100°C are summarized in Table II. From the Table, we see that the calculated concentration of the Fe_i species (Fe_i^+ and Fe_i^o) in the bulk region increases with increasing annealing temperature, while the FeB-pair concentration decreases. The reduction of the FeB-pair concentration is due to the pair dissociation as discussed earlier. In the surface region, no effect of Fe_i out-diffusion is observed during a 10-min annealing at 100°C. With increasing annealing temperatures, however, the Fe_i concentration in the surface region increases first and decreases after the annealing temperature exceeds the transition temperature. Similar to the bulk region, the concentration of the FeB pairs in the surface region exhibits a gradual decrease with increasing temperatures. In general, the calculated defect concentrations at 1.5 μm agrees well with the DLTS results. The pair binding energy derived from the isochronal annealing experiment,[11] in the temperature range between room temperature and 300°C, appears to be higher than a typical value of 0.58 eV, derived from the pairing reaction at temperatures close to room temper-

Table II. Summary of the results from the calculation based on E_b = 0.8 eV.

Temperature (°C)	$C_{Fe}(\infty)$	$C_{FeB}(\infty)$	C_{Fe}(1.5 μm)	C_{FeB}(1.5 μm)	C_{FeB}(DLTS)[a]	C_{Feb}(DLTS)[a]
	($\times 10^{13}$ cm^{-3})					
100	2.41	12.94	2.41	12.94	1.88	12.23
150	7.56	7.79	6.23	6.42	6.49	8.66
175	10.31	5.04	8.89	2.95	n/a	n/a
200	12.47	2.88	5.97	1.70	5.62	1.12
250	14.68	0.67	2.83	0.43	2.51	0.52
300	15.18	0.17	1.52	0.14	1.09	0.12

[a] Data from the DLTS measurements.
n/a not available.

ature (Table I). At the present time, no plausible explanation for the raising pair binding energy is available.

Summary and Conclusion

The reaction kinetics of iron-boron formation and dissociation in p-type silicon were investigated. Results indicate that the reaction kinetics depend strongly on the relative position of the ionization energy of interstitial iron and the Fermi level. At temperatures below a transition temperature where the ionization energy of interstitial iron is equal to the Fermi level, the iron-boron pairing reaction is dominated by the electrostatically enhanced recombination process between interstitial iron and substitutional boron. This pairing reaction is limited to iron diffusion and obeys first-order kinetics. The diffusion coefficient reported in the literature may be used to describe the diffusion process of the Fe_i^+ species during the pair recombination process. Based upon the present model, only one parameter (E_b) is required for calculation of the pairing reactions. The typical value of the pair binding energy derived from the pairing reaction at temperatures close to room temperature is on the order of 0.58 eV.

In the temperature range above the transition temperature, the thermal equilibrium between Fe_i^+ and Fe_i^o species, which is facilitated by the deionization of charged interstitial iron species, prevails. The observed reduction in the total Fe_i concentration during high temperature isochronal annealing is interpreted here as the result of Fe_i out-diffusion. Thus, the total concentration of the Fe_i species and FeB-pairs during an isochronal anneal may be assumed to remain unchanged during such an annealing process.

Manuscript submitted Oct. 28, 1991; revised manuscript received Oct. 1, 1992.

SEH America, Incorporated, assisted in meeting the publication costs of this article.

REFERENCES

1. A. Ohsawa, K. Honda, R. Takizawa, T. Nakanishi, M. Aoki, and N. Toyokura, in *Proceedings of the Sixth International Symposium on Silicon Materials Science and Technology, Semiconductor Silicon 1990,* H. R. Huff, K. G. Barraclough, and J.-i. Chikawa, Editors, PV 90-7, p. 601, The Electrochemical Society Softbound Proceedings Series, Pennington, NJ (1990).
2. H. H. Woodbury and G. W. Ludwig, *Phys. Rev.*, **117,** 102 (1960).
3. G. W. Ludwig and H. H. Woodbury, *Sol. Phys.*, **13,** 223 (1962).
4. Y. H. Lee, R. L. Kleinhenz, and J. W. Corbett, *Appl. Phys. Lett.*, **31,** 142 (1977).
5. K. Graff and H. Pieper, *This Journal,* **128,** 669 (1981).
6. K. Wunstel and P. Wagner, *Appl. Phys. A,* **27,** 207 (1982).
7. M. Suezawa and K. Sumino, in *Impurities, Defects and Diffusion in Semiconductors: Bulk and Layered Structures,* Vol. 163, D. J. Wolford, J. Bernholc, and E. E. Haller, Editors, p. 233, Materials Research Society, Pittsburgh (1990).
8. E. R. Weber, *Appl. Phys. A,* **30,** 1 (1983).
9. J. Utzig, *J. Appl. Phys.*, **65,** 3868 (1989).
10. T. Heiser and A. Mesli, *Appl. Phys. Lett.*, **58,** 2240 (1991).
11. L. C. Kimerling and J. L. Benton, *Physica,* **116B,** 297 (1983).
12. K. Kamiura, F. Hashimoto, and M. Yoneta, *This Journal,* **137,** 3642 (1990).
13. W. H. Shepherd and J. A. Turner, *J. Phys. Chem. Solids,* **23,** 1697 (1962).
14. H. Nakashima, T. Isobe, Y. Yamamoto, and K. Hashimoto, *Jpn. J. Appl. Phys.*, **27,** 1542 (1988).
15. L. C. Kimerling, J. L. Benton, and J. J. Rubin, *Inst. Phys. Conf. Ser.*, **59,** 217 (1981).
16. C. Kittel, *Introduction to Solid State Physics,* 2nd ed., John Wiley & Sons, Inc., New York (1960).
17. D. H. Navon, *Electronic Materials and Devices,* Houghton Mifflin Company, Boston (1975).
18. A. S. Grove, *Physics and Technology of Semiconductor Devices,* John Wiley & Sons, New York (1967).
19. C. D. Thurmond, *This Journal,* **122,** 1133 (1975).
20. K. Ryoo and W. E. Socha, *ibid.,* **138,** 1424 (1991).
21. G. Zoth and W. Bergholz, *J. Appl. Phys.*, **67,** 6764 (1990).
22. X. Gao, SEH America, Inc., Unpublished.
23. W. Wijaranakula, in *Defect Engineering in Semiconductor Growth, Processing and Device Technology,* S. Ashok, J. Chevallier, K. Sumino, and E. Weber, Editors, p. 561, Materials Research Society, Pittsburgh, PA (1992).